Broadband Phase Modulating System for White-Light Fourier Transformations

J. E. Stockley[a], S. A. Serati[a], D. Subacius[a], K. J. McIntyre[b] and K. F. Walsh[b]

[a] Boulder Nonlinear Systems, Inc. 450 Courtney Way Unit 107 Lafayette CO 80026

[b] Rochester Photonics Corporation, 330 Clay Road Rochester NY 146123

ABSTRACT

We discuss a white-light processing system that produces a dynamic, achromatic Fourier transformation over the visible spectrum. The system includes an achromatic Fourier transform lens system and a low-dispersion spatial light modulator.

A programmable phase mask can only write patterns with a spatial frequency appropriate for one wavelength. However, this problem is resolved by scaling broadband light from a point source to a common spatial frequency using an achromatic Fourier transformer. Then, the programmable phase mask must produce the same phase profile for all wavelengths. Using a chiral smectic liquid crystal (CSLC) spatial light modulator can minimize the wavelength dependence of the phase shifting elements. Phase modulation is accomplished by re-orientation of the optic axis in a plane transverse to the direction of propagation in a manner similar to mechanical rotation of a waveplate. The position of the optic axis is the same for all wavelengths and ideally so is the induced phase shift.

We present experimental far field diffraction patterns due to a CSLC spatial light modulator that produces a binary broadband phase mask and an achromatic Fourier transform lens system. An analog modulator is also introduced. Applications for this technology include optical processing, beam steering and adaptive optics.

Keywords: achromatic, Fourier, transform, chiral, smectic, liquid, crystal, gratings, broadband, phase

1. INTRODUCTION

White light Fourier transforms are of interest because incoherent processing in general reduces the noise associated with optical system imperfections over that of coherent systems[1]. In addition white-light transformation holds forth the promise of optical filtering and correlation based on spectral content. Broadband optical processing systems exhibit chromaticity due to the wavelength dependence of the phase filter and due to propagation to the far field. A similar problem occurs in steering broad band light and it has previously been suggested by Watson et. al.[2] that one solution is to use an achromatic Fourier transformer and an array of broadband phase shifters. We have previously analyzed the potential for broadband beam steering based on an implementation using an achromatic Fourier transformer and a low dispersion chiral smectic liquid crystal grating[3].

Propagation dispersion can be resolved by using an achromatic Fourier transformer. Spatially coherent achromatic Fourier transformers have been investigated in the past because of their unique treatment of broadband light[4,5]. This type of lens system scales broadband light from a common location in one focal plane to a common spatial resolution in another.

For real-time optical processing applications, a dynamic phase filter can be implemented using a spatial light modulator (SLM). Commonly used phase-only SLM technologies, employ optical path difference (OPD) modulation. For OPD modulation, the phase shift for different wavelengths becomes distorted, since the path length difference that produces a certain phase shift for red light is not the same path difference needed for blue light. That is, blue light is phase shifted more than red light by the same path difference. This is true for deformable mirrors as well as nematic liquid crystal devices. However, the problem is worse for nematic LC phase shifters, since the dispersion of the LC material amplifies the problem. For liquid crystal, the OPD is given by

$$OPD = \frac{2\pi\, n_e(V)\, d}{\lambda} \quad . \qquad (1)$$

Here $n_e(V)$ is the voltage induced change in the extraordinary index of refraction, d is the liquid crystal layer thickness and λ is the wavelength of the optical field.

As an example, Figure 1 shows how a linear phase profile becomes more disrupted as the OPD and LC material dispersion increases the phase error with decreasing wavelength. If the phase profile is an ideal linear ramp with modulo 2π resets, then at the design wavelength of the modulating elements (profile a) most of the energy is diverted into the first diffracted order. However, at other wavelengths (profiles b and c), more energy is scattered into higher spatial frequencies.

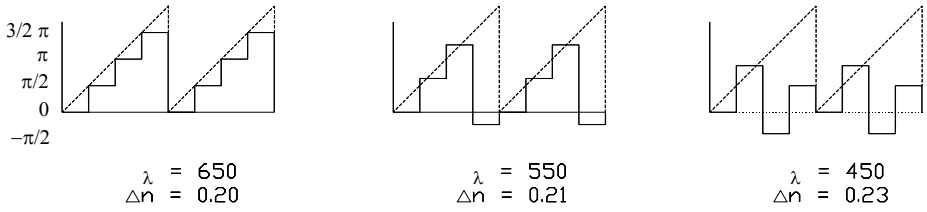

(a) (b) (c)

Figure 1. Wavelength-dependent, phase ramp profiles produced by a nematic liquid crystal phase-only modulator designed for operation at 650nm.

The wavelength dependence of a phase modulating SLM can be reduced by using a chiral smectic liquid crystal (CSLC) retarder as the modulating medium. These devices operate on the principle of polarization modulation. That is, manipulation of the polarization produces a change in optical phase. This polarization modulation is accomplished by re-orientation of the optic axis in a plane transverse to the direction of propagation in a manner similar to mechanical rotation of a waveplate. With a CSLC waveplate, the molecular tilt in the transverse plane changes as a function of applied electric field. This rotates the optic axis of the CSLC modulator. The position of the optic axis is the same for all wavelengths and ideally so is the induced phase shift.

Below, the performance of an achromatic Fourier transform (AFT) lens is presented. This is followed by the demonstration of dynamic achromatic Fourier transforms produced by a system comprised of the AFT and a low dispersion, binary switching, liquid crystal SLM. A low dispersion, analog phase SLM is introduced next, including design and proof of principle operation. Potential applications for this technology are discussed. Finally, these topics are summarized.

2. CHARACTERIZATION OF VISIBLE AFT LENS

An achromatic Fourier transform lens covering most of the visible spectrum has been fabricated. This AFT is based on a 3 lens, five element design discussed in Reference 3. The AFT was aligned so that the on-axis image point lies in the center of the exiting mechanical aperture. The alignment procedure involves adjusting the set screws and the incoming beam angle so that the image spot is centered for all wavelengths

across the bandwidth. The following test wavelengths were used (8 nm bandwidth): 535 nm, 564 nm, 593 nm, 622 nm, 650 nm.

The measured specifications are:

Design Spectral Band = 535 nm to 650 nm;

Focal length = 204.25 mm (at 593 nm);

Stop Diameter (located at the first lens surface) = 12 mm;

F-number = 19;

System Length = 695 mm.

After the lens was aligned, the following measurements were performed:

- Spot diameter for all test wavelengths (on-axis)
- Longitudinal chromatic aberration for all test wavelengths
- Lateral chromatic aberration for all test wavelengths using input gratings with periods of 540 μm, 108 μm and 42 μm
- Distortion using input gratings with periods of 540 μm, 108 μm and 42 μm

All of the measurements were performed by viewing the image spots through a microscope viewing system and translating the viewing stage using precision linear stages. The test gratings, linearly blazed and optimized for the visible region, were fabricated and replicated on BK7 blanks. The lateral position of the zeroeth order image spot served as the "on-axis" reference point for each grating to eliminate the effect of wedge in the substrate. Incidentally, the maximum observed image shift due to substrate wedge for all gratings was 25 microns.

The spot diameter was measured for a 12 mm diameter input aperture. This provides a lens F-number of 19 and implies an Airy diameter of 25 microns @ 593 nm. No grating was present during these measurements. The spot diameter was measured from zero intensity points. The measurement error is estimated to be +/- 0.005 mm. Refer to Figure 2.

Wavelength (nm)	Spot diameter (mm)
535	0.027
564	0.030
593	0.030
622	0.029
650	0.030

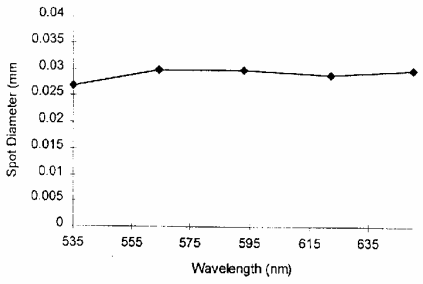

Figure 2. Spot diameter at focus for each test wavelength.

The longitudinal position of best focus was measured for all wavelengths. The positions shown below in Figure 3 are relative to the middle wavelength, 593nm. No grating was present during these measurements. The measurement error is estimated to be +/- 0.075 mm.

Wavelength (nm)	Longitudinal chromatic aberration* (mm)
535	+0.559
564	+0.229
593	0.000
622	-0.114
650	-0.343

* Results are positions relative to that of 593 nm. Negative is towards the lens, positive is away from the lens

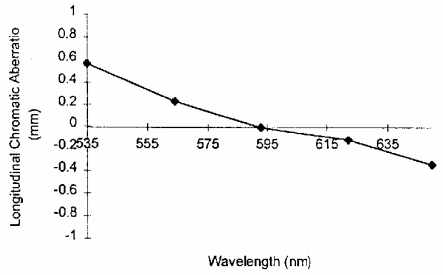

Figure 3. Longitudinal chromatic aberration.

The lateral image spot position was measured for all wavelengths and for three different grating periods. The positions shown in Figure 4 below are relative to the middle wavelength, 593 nm. The measurement error is estimated to be +/- 0.005 mm.

Lateral chromatic aberration* (mm)

Wavelength (nm)	Period = 540 um	Period = 108 um	Period = 42 um
535	0.000	+0.001	-0.004
564	0.000	-0.001	-0.003
593	0.000	0.000	0.000
622	-0.001	+0.001	0.000
650	-0.004	+0.001	0.000

* Results are positions relative to that of 593 nm. Negative is towards the optical axis, positive is away from the optical axis

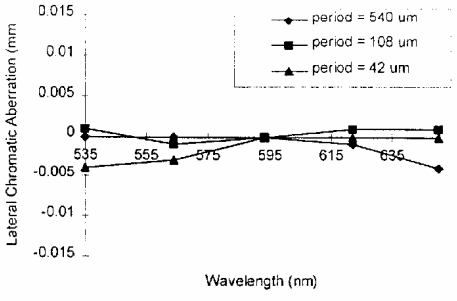

Figure 4. Lateral chromatic aberration.

The distortion was measured for three different grating periods. An ideal Fourier transform lens obeys the following relation for lateral image position: $y = f\sin\theta$, where y is the image height, f is the focal length, and θ is the input beam angle. Therefore, the distortion error for such a lens can be expressed as, $Error_{distortion} = y_{actual} - f\sin\theta$, where y_{actual} is the actual or measured image height. The table accompanying Figure 5 shows the actual image height for λ = 593 nm and the resulting distortion error for a focal length of 204.25 mm. This calibrated focal length minimizes the peak to valley distortion error as a function of image height (or equivalently grating period). The image height measurement error is estimated to be +/- 0.015 mm.

Grating Period (um)	Input angle (deg)	Ideal image height (mm) focal length = 204.25 mm	Measured image height (mm)	Distortion Error (mm)
540	0.0629	0.224	0.229	+0.005
108	0.3146	1.121	1.130	+0.009
42	0.8090	2.884	2.875	-0.009

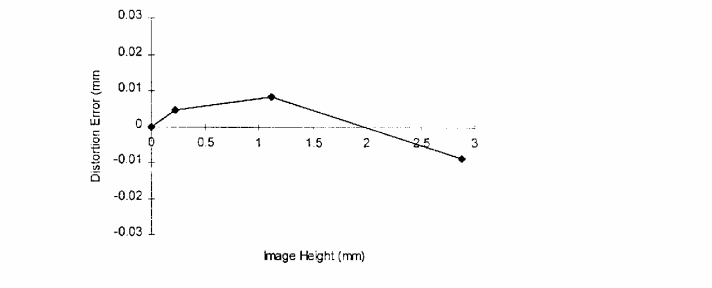

Figure 5. Distortion error for achromatic Fourier transform lens.

Based on the measurements provided, the performance of this lens is excellent. All of the measured quantities are equal to the targeted values to within the associated measurement errors except for longitudinal chromatic aberration. This is not expected to present a problem as the spot size does not vary appreciably through focus. The depth of focus for a 7.82 mm input diameter aperture (same as the SLM) is approximately +/-0.800 mm which encapsulates the range of the measured values. The accuracy of the lateral placement of the spots is at least one-half of one spot width for all wavelengths and grating periods tested.

3. BINARY SPATIAL LIGHT MODULATOR

The key to producing a broadband dynamic Fourier transform is a low dispersion spatial light modulator. A liquid crystal grating which produces binary phase achromatically at visible wavelengths is accomplished using a CSLC (chiral smectic liquid crystal) SLM (spatial light modulator) of 256x256 pixels which is a zero order quarter-wave retarder at 570 nm. On reflection, this device acts as a rotative half-wave plate. The pixel pitch is 21 μm. Consequently the minimum grating period is 42 μm. The SLM modulates the light using polarization manipulation. For the case considered here linearly polarized light was incident on the SLM. Depending on the SLM's optic axis with respect to the incident polarization, it acts as a binary amplitude or phase modulator. For amplitude modulation, the CSLC optic axis is either parallel to the incident polarization (producing a bright state) or at 45^o (resulting in a 90^o rotation of the polarization and a dark state). For binary phase modulation, the optic axis of the CSLC alternates between orientations of 22.5^o and 67.5^o with respect to the incident polarization yielding 0 and π radians of phase, respectively. This device can operate at 1000 frames per second.

4. BROADBAND SYSTEM DEMONSTRATION FOR VISIBLE LIGHT

The test configurations for demonstrating achromatic Fourier transformations of broadband phase patterns are shown in Figure 6. Figure 6(a) shows the set-up with standard output coupling lenses. These are used to produce a wavelength dependent Fourier transform at a focal point of 204 mm. The focal point is chosen

so that the two-lens combination will produce the same magnification as the achromatic Fourier transform lens. To achieve this focal length, two 250 mm focal length lenses were placed 194 mm apart. In Figure 6 (b), The AFT lens replaces the two chromatic output lenses.

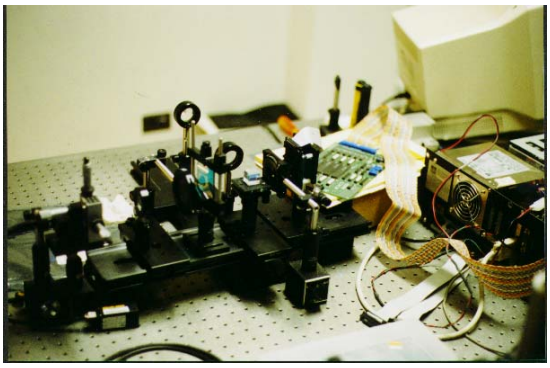

(a)

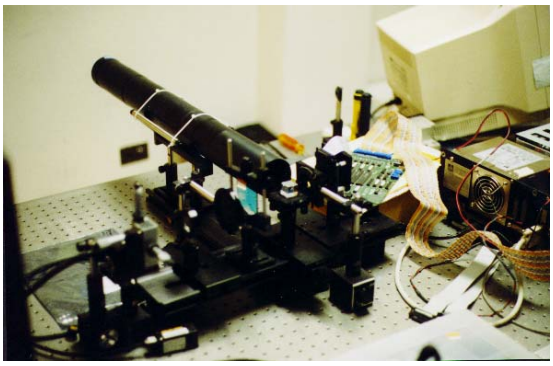

(b)

Figure 6. Test configurations for the system demonstration using components that operate over the visible spectrum. (a) System with standard output lenses. (b) System with AFT lens.

For this demonstration, a broadband binary SLM is used to generate grating patterns. The SLM is illuminated with a plane wave from a broadband source. The broadband plane wave is generated by spatially filtering a thermal source and collimating the filtered light. An IR-cut filter is used to limit the spectral band to visible wavelengths (400 nm to 650 nm). This light is then polarized and reflected onto the SLM using a broadband polarizing beam cube.

After the polarized light passes through the beam cube, it is then correctly aligned with the optic axis of the SLM using a passive rotatable half-wave plate in front of the SLM. For binary phase modulation, the input light's polarization is made to bisect the SLM's rotation angle, as discussed above. If the passive half-wave plate is rotated ± 11.25 degrees, a binary amplitude pattern is generated instead of a phase pattern. This occurs because the incident polarization is now aligned parallel to the optic axis of the CSLC modulator when the SLM is in one of its two states. The light reflected from the SLM passes back through the passive half-wave plate. When the light is reflected back through the half-wave plate, the waveplate's rotation is cancelled which re-aligns the light's polarization to the beam cube. This arrangement allows the modulated component of the reflected light to pass through the polarizing beam cube producing a broadband pattern at the front focal plane of the (a) output lenses or (b) the achromatic Fourier transform lens. The unmodulated component is reflected by the beam cube back into the source. After exiting the polarizing beam cube, the modulated light is processed by either the two output lenses or the AFT, depending on the set-up.

Figure 7 shows photographs of the far field patterns for a binary phase grating of period 42 μm. In 7 (a) the output is taken from the chromatic coupling lenses of the set-up in Figure 6 (a). While for 7 (b), the grating dispersion is corrected by the AFT lens of set-up 6 (b). In fact, the far field pattern of Figure 7 (b) shows that the AFT lens actually overcompensates slightly. (Red is now somewhat closer to the zero order.) Recall that the AFT was optimized for a BK7 grating which operates on the principle of optical path difference. Since the phase reset of the SLM is broadband, the modulation dispersion is absent and the far field pattern is slightly over-corrected. In both 7(a) and 7(b) a secondary blue-green spot appears near and just below the zero order. This spot is a reflection from the beam splitter cube.

With an achromatic Fourier transform lens the grating dispersion is corrected causing the diffracted orders to be focussed to a dot, as in 7 (b), instead of a dash, seen in 7 (a). The AFT is actually a lens system consisting of several elements. This lens system uses diffractive and refractive components to create different magnifications between common focal planes for the spectral components within broadband light. This wavelength-dependent scaling (or lateral color) eliminates the dispersion caused by the grating pattern and thus produces wavelength-independent spatial distributions for the transform. Figure 7 demonstrates that this arrangement operates as described.

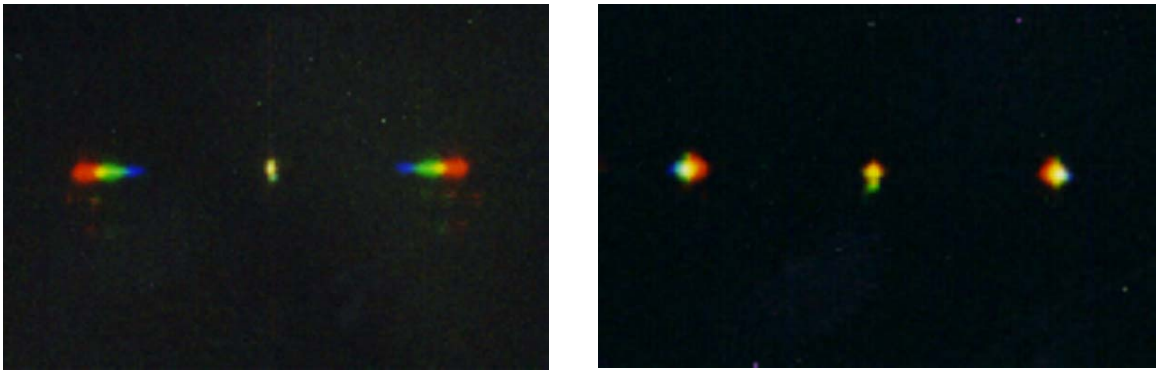

(a) (b)

Figure 7. Photographs of the far field diffraction pattern for a 42 μm period binary phase grating. (a) grating dispersion is present. (b) the AFT compensates for grating dispersion.

Because of the dynamic range of photographic film, the zero order diffraction is enhanced in Figure 7. Figure 8 shows the 256 level thermal prints corresponding to the far field patterns of Figure 7. Note that the thermal prints clearly demonstrate an insignificant intensity in the undiffracted zero order compared to the first order.

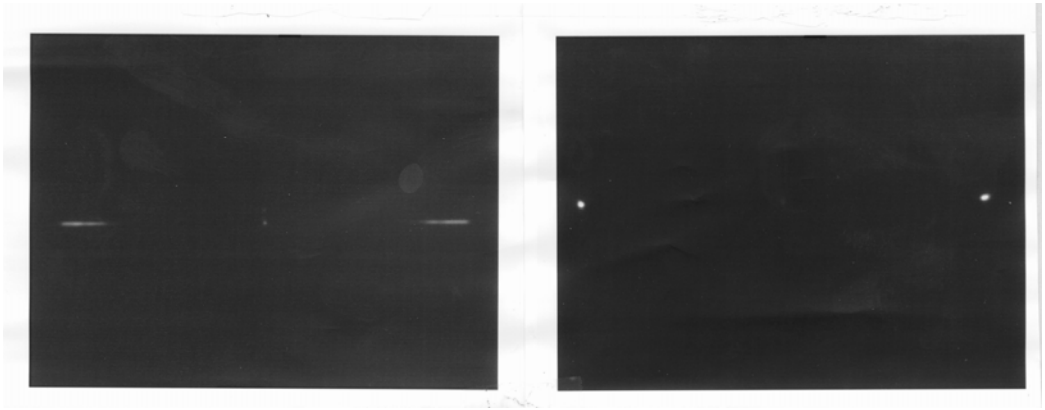

Figure 8. Thermal prints of the diffraction patterns in Figure 7. Note that the zero order is almost non-discernable in the 256 level thermal prints of the phase grating far field diffraction patterns.

These results demonstrate that the CSLC modulator produces a wavelength-independent phase shift, since the remnant central order is small even though the illumination is broadband, which is evident from the grating dispersion visible in the uncompensated diffracted orders (left side).

Figure 9 shows photographs of the dispersive and corrected far field diffraction patterns corresponding to a checker board pattern written to the SLM. These photos demonstrate that the AFT lens corrects grating dispersion regardless of azimuth. The checker board pattern is not perfectly symmetric, which results in a significant amount of undiffracted light in the zero order.

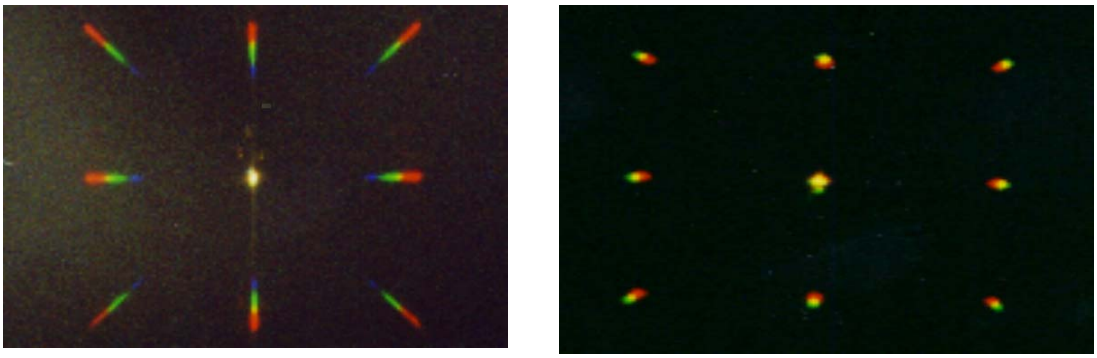

(a) (b)

Figure 9. Photographs of the far field patterns for a checker board written to the SLM. (a) Grating dispersion is present for the two-lens set-up of Figure 6 (a). (b) Grating dispersion has been corrected by the AFT lens.

5. ANALOG PHASE SPATIAL LIGHT MODULATOR

One obvious improvement to the system would be extension of the non-dispersive phase modulation to analog operation with a modulation depth of up to 2π. To achieve such a modulation depth using a topological phase shift requires a reflection mode device with an optic axis reorientation of 90 degrees[3].

A cross section of a sub-millisecond 2π phase-only modulator is shown below. This modulator requires a high-voltage backplane that has highly-reflective mirrors over the pixels and is optically flat over the area of the array. Above the mirrors is a passive quarter-wave retarder which preserves the handedness of the circularly polarized light incident on the modulator. This passive retarder is a polymer nematic liquid crystal (PNLC). A barrier layer separates the polymer LC from the active half-wave retarder. This barrier layer is a thin passivation that protects the solid nematic material from being dissolved by the CSLC that is used for the active wave-plate.

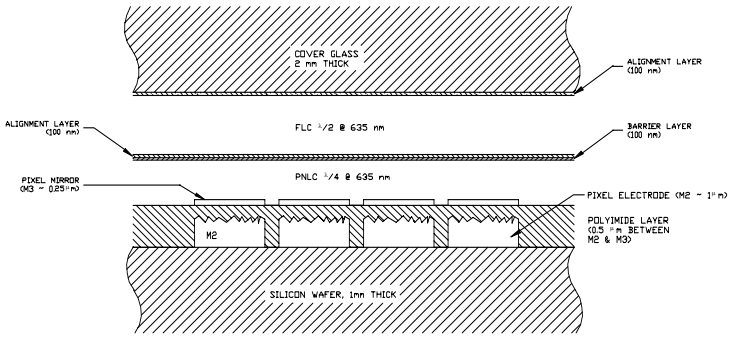

Figure 10. Scale drawing of the 2π CSLC modulator on a VLSI backplane.

The phase modulator design presented above requires a rotative half-wave CSLC retarder. As mentioned above, this CSLC retarder should ideally have a full molecular rotation angle of 90° to provide a full 2π phase shift. The molecular tilt is a function of the material being used. The only CSLC that has sufficient tilt is a chiral smectic C (SmC*) material.

It is a common belief that SmC* materials are inappropriate for analog SLMs, because despite their large tilt angles and low voltage requirements, their switching tends to be binary in nature. However, it is now known and has been demonstrated that certain SmC* materials exhibit a controllable analog optical response[6,7].

A fixed quarter-wave retarder comprised of a polymer nematic liquid crystal (PNLC) was fabricated onto a VLSI backplane. Next this device was gapped using two micron spacers and filled with a high-tilt CSLC. Switching the VLSI backplane as a single pixel device yields an estimate of the required applied voltage. The device tested was a 128x128 SLM backplane. The PNLC film was approximately 1 micron thick and the CSLC reflected a blue color when the device was placed beneath a polarizer, indicating a half-wave of retardation in the red.

A Plot of the optical response for a 1 Hz square wave applied to the integrated modulator is shown in Figure 11 below. The integrated modulator consists of VLSI backplane, passive PNLC λ/4 retarder, active CSLC λ/2 retarder and ITO-coated coverglass. The 78 degrees of optic axis reorientation translate to a phase modulation depth of 312 degrees. This is enough to implement 7 uniformly spaced quantized phase levels. The CSLC used has a theoretical maximum reorientation of 86 degrees, but materials exist which can reorient by as much as 96 degrees.

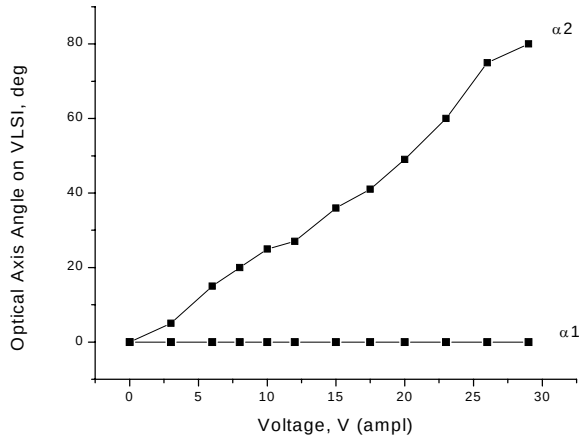

Figure 11. Optic axis orientation as a function of applied voltage at 1 Hz. Here the integrated modulator is configured to switch as a single pixel. Orientation of the optic axis relative to the zero field state is denoted by α1 or α2, each representing a different polarity.

6. POTENTIAL APPLICATIONS OF THIS TECHNOLOGY

Optical processing and beam steering are just two possible areas of application for this technology. Other possibilities include communications, diffractive and adaptive optics. For routing data packets in a wavelength division multiplexing (WDM) system, an array of non-dispersive phase shifters could be used to reduce crosstalk between channels. In adaptive optics, the goal is to correct the wavefront of the optical signal allowing the broadband light to be correctly imaged. If the adaptive optical system is diffractive, the spectral components separate, blurring the image. However, this effect is correctable using the achromatic Fourier transformer if the phase shifter is not dispersive. For a phase shifter that is dispersive, no one has found a method for correcting the problem except by limiting the diffraction to very small angles (i.e. limiting the resolution of the adaptive optics). Applications for adaptive optics are increasing beyond telescope imaging systems where large deformable mirrors are used to correct the effects of atmospheric turbulence. For example, adaptive optics are being considered for medical imaging systems where the image is distorted by body fluids. There are many of these types of applications, if the adaptive optics have

the speed and resolution to perform the task and the cost is not prohibitive.

7. SUMMARY AND CONCLUSIONS

A broadband dynamic Fourier transform system has been discussed. The design of the system calls for an array or grid of non-dispersive phase shifters and an achromatic Fourier transform (AFT) lens. An SLM which uses polarization modulation to diffract incident light followed by an AFT has demonstrated broadband characteristics. Extension of the non-dispersive phase modulator technology to analog operation has begun. We have mentioned a few of several potential applications for this technology.

8. ACKNOWLEDGMENTS

This work is supported in part by Wright Laboratory, Wright-Patterson AFB contract numbers F33615-96-C-1965, and F33615-97-C-1162. Portions of this research were also funded by Phillips Laboratory, Kirtland AFB, contract number F29601-98-C-0045, and NASA Johnson Space Center, contract number NAS9-98082.

9. REFERENCES

1. F. T. S. Yu, "Color Image Processing," in Optical Signal Processing, J.J. Horner, ed. (Academic Press New York, 1987) pages 3-21.

2. E. A. Watson, P. F. McManamon, L. J. Barnes, and A. J. Carney, "Applications of dynamic gratings to broad spectral band beam steering," SPIE Vol. 2120 Laser Beam Propagation and Control (1994).

3. J. E. Stockley, S. A. Serati, G. D. Sharp, P. Wang, K. F. Walsh, and K. M. Johnson, “Broadband Beam Steering,” SPIE Vol. 3131 Optical Scanning Systems: Design and Applications (1997).

4. G. M. Morris, "Diffraction Theory for an achromatic Fourier transformation," Appl. Opt. Vol. 20 2017-2025, (1981)

5. G. M. Morris, and D. A. Zweig, "White Light Fourier Transforms," in Optical Signal Processing, J.J. Horner, ed. (Academic Press New York, 1987) pages 23-70.

6. S. A Serati, G. D. Sharp, R. A. Serati, D. J. McKnight, and J. E. Stockley, “128x128 analog liquid crystal spatial light modulator,” SPIE Vol. 2490 Optical Pattern Recognition VI (1995).

7. J. E. Stockley, G. D. Sharp, S. A. Serati, and K. M. Johnson, "Analog optical phase modulator based on chiral smectic and polymer cholesteric liquid crystals," Opt. Lett. Vol. 20 2441-2443, (1995).